

# Design, Synthesis, and Bioevaluation of Novel Strobilurin Derivatives<sup>†</sup>

Zhu, Xiaolei(朱晓磊)   Wang, Fu(王福)   Li, Hui(李慧)   Yang, Wenchao(杨文超)  
Chen, Qiong(陈琼)   Yang, Guangfu\*(杨光富)

Key Laboratory of Pesticide and Chemical Biology of Ministry of Education, College of Chemistry, Central China Normal University, Wuhan, Hubei 430079, China

Strobilurins are one of the most important natural products with fungicidal activities and well known for their novel action mode, broad fungicidal spectrum, lower toxicity against mammalian cells, and environmentally benign characteristics. Design and syntheses of strobilurin analogues therefore have attracted great attention in the field of agrochemistry. Previously, we successfully developed a new molecular design method of pharmacophore-linked fragment virtual screening (PFVS) and discovered a lead compound (*E*)-methyl-2-(2-(((3-(imino(phenyl)-methyl)phenyl)thio)methyl)phenyl)-3-methoxyacrylate (**1**). To discover new strobilurin analogues with higher fungicidal activity, the structural modification of compound **1** was carried out guided by bioisosterism. A series of benzophenone derivatives **2a–2j** were synthesized, among which compound **2j** with a  $K_i$  value of 1.89 nmol/L was identified as the most promising inhibitor of porcine cytochrome  $bc_1$  complex, 157-fold improved binding affinity compared to the commercially available  $bc_1$  inhibitor Azoxystrobin (AZ). In addition, most of the new compounds displayed excellent fungicidal activity against *Sphaerotheca fuliginea* at the concentration of 200  $\mu$ mol/L. The present work indicates that strobilurin analogues containing benzophenone side chains may be the ideal leads for future fungicide discovery.

**Keywords** strobilurin, cytochrome  $bc_1$  complex, benzophenone, bioisosterism

## Introduction

Cytochrome  $bc_1$  complex (EC 1.10.2.2,  $bc_1$ ), also known as Complex III, is an essential component of the cellular respiratory chain or the photosynthetic apparatus in photosynthetic bacteria. It catalyzes the electron transfer from quinol to a soluble cytochrome *c* (cyt *c*) and couples this electron transfer to the translocation of protons across the membrane, generating the proton gradient required for ATP biosynthesis.<sup>[1–4]</sup> Inhibition of the function of  $bc_1$  complex would block the electron transfer and cause serious problem even death to the organism, which makes inhibitors targeting  $bc_1$  complex become a significant area in fungicides discovery.

Among the existing  $bc_1$  complex inhibitors specifically binding to the  $Q_o$  site, strobilurins derivatives have attracted the greatest attention due to the broad spectrum and efficient activity. Since the first commercialized products azoxystrobin and kresoxim-methyl (Figure 1) were launched in 1996, thousands of analogues with diverse structure<sup>[5–7]</sup> have been synthesized and over 10 strobilurin fungicides are available for field application. However, the widespread application of strobilurin fun-

gicides has led to the rapid development of resistance in a range of important plant pathogens.<sup>[8,9]</sup> Developing novel strobilurin analogues may overcome this problem and has attracted much attention from agricultural chemists in recent years.

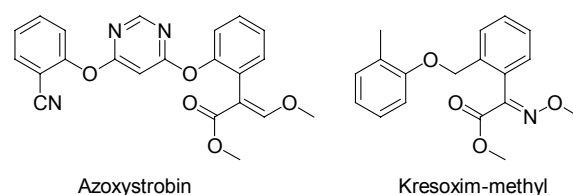


**Figure 1** Structures of commercialized products azoxystrobin and kresoxim-methyl.

Recently, we developed a new molecular design method of pharmacophore-linked fragment virtual screening (PFVS),<sup>[10]</sup> which produced a new lead compound (*E*)-methyl-2-(2-(((3-(imino(phenyl)-methyl)phenyl)thio)methyl)phenyl)-3-methoxyacrylate (**1**) as shown in Figure 2. Unfortunately, although compound **1** was successfully synthesized, it was found to be unstable

\* E-mail: gfyang@mail.ccnu.edu.cn

Received June 24, 2012; accepted August 6, 2012.

Supporting information for this article is available on the WWW under <http://dx.doi.org/10.1002/cjoc.201200607> or from the author.

<sup>†</sup> Dedicated to the 80th Anniversary of Chinese Chemical Society.

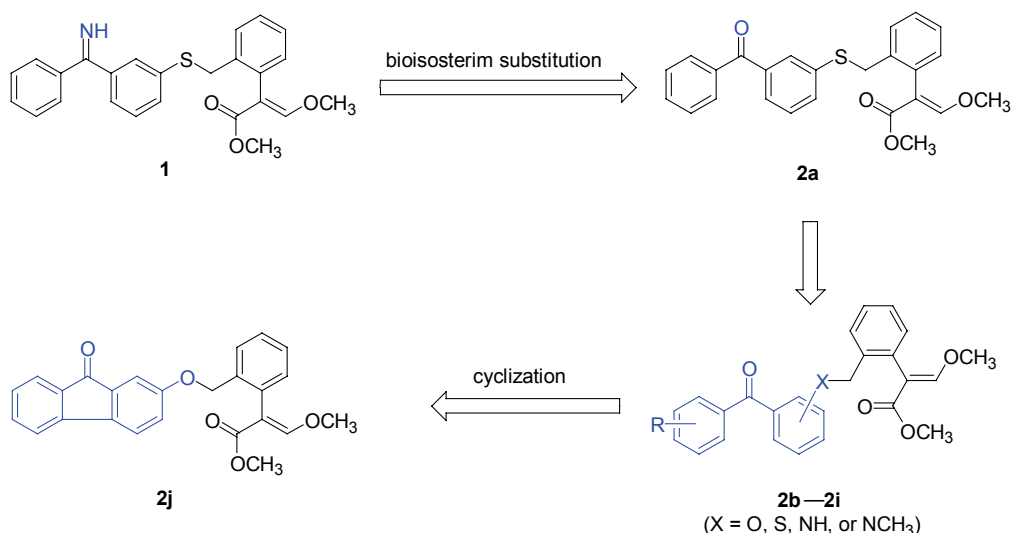
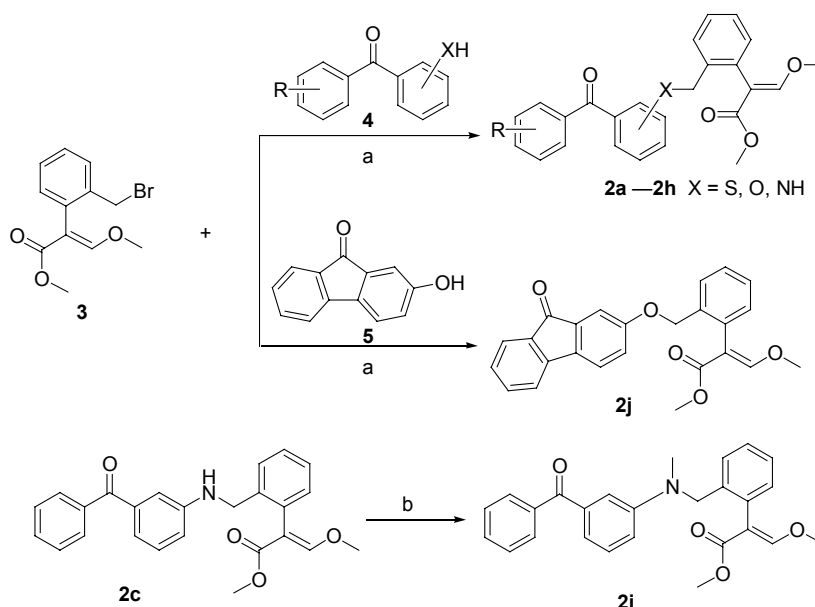


**Figure 2** Structural optimization of lead compound **1**.

**Scheme 1** Synthetic route for the newly designed compounds **2a–2j**



**Reagent and conditions:** (a) K<sub>2</sub>CO<sub>3</sub>, acetone, reflux; (b) K<sub>2</sub>CO<sub>3</sub>, CH<sub>3</sub>I, acetone, reflux

due to the existence of the imino. We also found that its *N*-methylated derivatives were unstable. Because oxygen is the classical bioisosterim of NH, we therefore designed compound **2a**, whose *K<sub>i</sub>* value against porcine cytochrome *bc*<sub>1</sub> complex was determined to be 13.95 nmol/L. This result prompted us to study the potential of the benzophenone-containing strobilurin derivatives as inhibitors of cytochrome *bc*<sub>1</sub> complex. In fact, as a critical intermediate in the biosynthetic pathway of flutriafol,<sup>[11]</sup> benzophenone has demonstrated a diverse array of pharmacological activities, such as antifungal activities. However, to the best of our knowledge, no benzophenone-containing strobilurin analogues have been reported so far. Herein, nine benzophenone-containing strobilurin derivatives with different linking modes between benzophenone and the pharmacophore

of  $\beta$ -methoxyacrylate were synthesized and assayed. Finally, a fluorenone-containing strobilurin derivative **2j** was designed and synthesized by the cyclization strategy. Very interestingly, compound **2j** with a *K<sub>i</sub>* value of 1.89 nmol/L was identified as the most promising inhibitor of porcine cytochrome *bc*<sub>1</sub> complex. Further *in vivo* evaluation results revealed that compounds **2b**, **2g** and **2j** showed good fungicidal activity against *Sphaerotheca fuliginea* at the concentration of 200  $\mu$ mol/L.

## Experimental

Unless otherwise noted, all chemical reagents were commercially available and treated with standard methods before use. Silica gel column chromatography

(CC): silica gel (200—300 mesh; Qingdao Makall Group Co., Ltd., Qingdao, China). Solvents were dried in a routine way and redistilled.  $^1\text{H}$  and  $^{13}\text{C}$  spectra were recorded in  $\text{CDCl}_3$  or  $d_6$ -DMSO on a Varian Mercury 600 or 400 spectrometer and resonances ( $\delta$ ) are given relative to tetramethylsilane (TMS). The following abbreviations were used to designate chemical shift multiplicities: s = singlet, d = doublet, t = triplet, m = multiplet, br = broad. High Resolution Mass Spectra (HRMS) were acquired in positive mode on a WATERS MALDI SYNAPT G2 HDMS (MA, USA). Melting points were taken on a Buchi B-545 melting point apparatus and uncorrected. Intermediates **4** and **5** were purchased from Sigma-Aldrich.

#### General procedure for the synthesis of target compounds **2a—2h** and **2j**

To a mixture of anhydrous  $\text{K}_2\text{CO}_3$  (0.82 g, 6.0 mmol) in dry acetone (20 mL), 5.0 mmol of intermediate **4** or 2-hydroxy-9H-fluoren-9-one (**5**) was added, then the resulted mixture was stirred and refluxed for 0.5 h. Then, the intermediate of (*E*)-methyl-2-(2-(bromomethyl)-phenyl)-3-methoxyacrylate **3** (1.42 g, 5.0 mmol) was added into the solution, the reaction mixture was stirred for a further 5—8 h under reflux. The resulting mixture was cooled to room temperature and filtered off by suction, and the solvent was evaporated to give the crude product, followed by chromatography purification on silica using a mixture of petroleum ether and ethyl acetate (10 : 1) as eluent to give the target compounds **2a—2h** and **2j** in yields of 65%—81%.

#### General procedure for the synthesis of target compounds (**2i**)

To a mixture of 5.0 mmol compound **2c** in dry acetone (20 mL), anhydrous  $\text{K}_2\text{CO}_3$  (1.38 g, 10 mmol) and  $\text{CH}_3\text{I}$  (1.42 g, 10 mmol) were added respectively, stirred and refluxed for 2 h. The resulting mixture was cooled to room temperature and filtered off by suction, and the solvent was evaporated to give the crude product, followed by chromatography purification on silica using a mixture of petroleum ether and ethyl acetate (6 : 1) as eluent to give the target compounds **2i**.

**(E)-Methyl-2-(2-(((3-benzoylphenyl)thio)methyl)-phenyl)-3-methoxyacrylate (2a)** Yield 81%. Yellow oil.  $^1\text{H}$  NMR (600 MHz,  $d_6$ -DMSO)  $\delta$ : 3.65 (s, 3H,  $\text{COOCH}_3$ ), 3.78 (s, 3H,  $=\text{CH-OCH}_3$ ), 4.04 (s, 2H,  $\text{CH}_2$ ), 7.13 (d,  $J=7.2$  Hz, 1H, Ar-H), 7.21—7.23 (m, 1H, Ar-H), 7.25—7.27 (m, 1H, Ar-H), 7.31—7.35 (m, 2H, Ar-H), 7.45—7.47 (m, 3H, Ar-H), 7.57—7.59 (m, 3H, Ar-H), 7.66 (s, 1H,  $=\text{CH-OCH}_3$ ), 7.71—7.72 (m, 2H, Ar-H);  $^{13}\text{C}$  NMR (100 MHz,  $d_6$ -DMSO)  $\delta$ : 195.1, 167.0, 160.6, 137.6, 137.2, 136.7, 135.8, 133.0, 132.6, 132.4, 131.4, 129.6, 129.3, 129.0, 128.9, 128.4, 127.4, 127.1, 126.9, 109.1, 61.6, 51.1, 36.5; HRMS (MALDI) calcd for  $\text{C}_{25}\text{H}_{22}\text{O}_4\text{S}$   $[\text{M} + \text{Na}]^+$  441.1131, found 441.1107.

**(E)-Methyl-2-(2-((3-benzoylphenoxy)methyl)phenyl)-**

**3-methoxyacrylate (2b)** Yield 77%. White solid, m.p. 80—81 °C.  $^1\text{H}$  NMR (600 MHz,  $\text{CDCl}_3$ )  $\delta$ : 3.67 (s, 3H,  $\text{COOCH}_3$ ), 3.79 (s, 3H,  $=\text{CH-OCH}_3$ ), 5.02 (s, 2H,  $\text{CH}_2$ ), 7.13 (d,  $J=6.6$  Hz, 1H, Ar-H), 7.18 (d,  $J=7.2$  Hz, 1H, Ar-H), 7.32—7.35 (m, 5H, Ar-H), 7.44—7.46 (m, 2H, Ar-H), 7.53 (d,  $J=6.6$  Hz, 1H, Ar-H), 7.56—7.57 (m, 2H,  $=\text{CH-OCH}_3$  and Ar-H), 7.77 (d,  $J=7.8$  Hz, 2H, Ar-H);  $^{13}\text{C}$  NMR (100 MHz,  $d_6$ -DMSO)  $\delta$ : 195.2, 166.8, 160.5, 158.1, 138.3, 136.8, 135.4, 132.5, 132.0, 131.1, 129.6, 129.4, 128.4, 127.4, 122.1, 119.1, 115.2, 108.7, 67.7, 61.7, 51.1; HRMS (MALDI) calcd for  $\text{C}_{25}\text{H}_{22}\text{O}_5$   $[\text{M} + \text{Na}]^+$  425.1359, found 425.1340.

**(E)-Methyl-2-(2-(((3-benzoylphenyl)amino)-methyl)phenyl)-3-methoxyacrylate (2c)** Yield 75%. Yellow oil.  $^1\text{H}$  NMR (600 MHz,  $d_6$ -DMSO)  $\delta$ : 3.59 (s, 3H,  $\text{COOCH}_3$ ), 3.79 (s, 3H,  $=\text{CH-OCH}_3$ ), 4.09 (d,  $J=5.4$  Hz, 2H,  $\text{CH}_2$ ), 6.52—6.54 (m, 1H, Ar-H), 6.72 (d,  $J=7.8$  Hz, 1H, Ar-H), 6.82 (d,  $J=7.2$  Hz, 1H, Ar-H), 6.88 (s, 1H, NH), 7.05 (d,  $J=7.2$  Hz, 1H, Ar-H), 7.17—7.22 (m, 2H, Ar-H), 7.23—7.26 (m, 1H, Ar-H), 7.33 (d,  $J=7.8$  Hz, 1H, Ar-H), 7.48—7.51 (m, 2H, Ar-H), 7.61—7.64 (m, 1H, Ar-H), 7.66—7.67 (m, 3H,  $=\text{CH-OCH}_3$  and Ar-H);  $^{13}\text{C}$  NMR (100 MHz,  $d_6$ -DMSO)  $\delta$ : 196.1, 167.0, 160.6, 148.6, 138.0, 137.6, 137.3, 132.3, 131.7, 130.9, 129.4, 128.9, 128.3, 127.4, 126.2, 126.1, 117.2, 115.9, 112.7, 108.9, 61.7, 51.2, 44.0; HRMS (MALDI) calcd for  $\text{C}_{25}\text{H}_{23}\text{NO}_4$   $[\text{M} + \text{Na}]^+$  424.1519, found 424.1520.

**(E)-Methyl-2-(2-((2-benzoylphenoxy)ethyl)phenyl)-3-methoxyacrylate (2d)** Yield 70%. Yellow oil.  $^1\text{H}$  NMR (600 MHz,  $\text{CDCl}_3$ )  $\delta$ : 3.68 (s, 3H,  $\text{COOCH}_3$ ), 3.79 (s, 3H,  $=\text{CH-OCH}_3$ ), 4.89 (s, 2H,  $\text{CH}_2$ ), 6.89 (d,  $J=8.4$  Hz, 2H, Ar-H), 7.02—7.05 (m, 1H, Ar-H), 7.07—7.11 (m, 2H, Ar-H), 7.19—7.21 (m, 1H, Ar-H), 7.37—7.40 (m, 1H, Ar-H), 7.41—7.46 (m, 3H, Ar-H), 7.55—7.57 (m, 2H, Ar-H and  $=\text{CH-OCH}_3$ ), 7.84 (d,  $J=7.8$  Hz, 2H, Ar-H);  $^{13}\text{C}$  NMR (100 MHz,  $d_6$ -DMSO)  $\delta$ : 195.8, 166.7, 161.0, 155.6, 137.5, 135.3, 133.1, 132.0, 130.8, 130.7, 129.1, 128.9, 128.7, 128.6, 127.1, 126.8, 125.8, 120.7, 112.9, 108.1, 67.2, 61.8, 51.2; HRMS (MALDI) calcd for  $\text{C}_{25}\text{H}_{22}\text{O}_5$   $[\text{M} + \text{Na}]^+$  425.1359, found 425.1733.

**(E)-Methyl-2-(2-((3-benzoylphenoxy)methyl)-phenyl)-3-methoxyacrylate (2e)** Yield 77%. Yellow oil.  $^1\text{H}$  NMR (600 MHz,  $d_6$ -DMSO)  $\delta$ : 3.62 (s, 3H,  $\text{COOCH}_3$ ), 3.82 (s, 3H,  $=\text{CH-OCH}_3$ ), 5.03 (s, 2H,  $\text{CH}_2$ ), 7.06 (d,  $J=8.4$  Hz, 2H, Ar-H), 7.15 (d,  $J=5.4$  Hz, 1H, Ar-H), 7.30—7.33 (m, 2H, Ar-H), 7.49—7.50 (m, 1H, Ar-H), 7.52—7.54 (m, 2H, Ar-H), 7.62—7.64 (m, 1H, Ar-H), 7.67—7.69 (m, 3H, Ar-H and  $=\text{CH-OCH}_3$ ), 7.73 (d,  $J=8.4$  Hz, 2H, Ar-H);  $^{13}\text{C}$  NMR (100 MHz,  $d_6$ -DMSO)  $\delta$ : 194.4, 167.0, 162.0, 160.8, 137.7, 135.2, 132.2, 132.1, 131.2, 129.5, 129.3, 128.4, 127.7, 127.67, 127.62, 114.5, 108.7, 67.9, 61.9, 51.3; HRMS (MALDI) calcd for  $\text{C}_{25}\text{H}_{22}\text{O}_5$   $[\text{M} + \text{Na}]^+$  425.1359, found 425.1373.

**(E)-Methyl-2-(2-((3-(2-fluorobenzoyl)phenoxy)-methyl)phenyl)-3-methoxyacrylate (2f)** Yield 69%.

Yellow oil.  $^1\text{H}$  NMR (600 MHz,  $\text{CDCl}_3$ )  $\delta$ : 3.70 (s, 3H,  $\text{COOCH}_3$ ), 3.82 (s, 3H,  $=\text{CH-OCH}_3$ ), 5.05 (s, 2H,  $\text{CH}_2$ ), 6.93–6.95 (m, 2H, Ar-H), 7.13–7.16 (m, 1H, Ar-H), 7.18–7.19 (m, 1H, Ar-H), 7.23–7.24 (m, 1H, Ar-H), 7.33–7.35 (m, 2H, Ar-H), 7.48–7.51 (m, 3H, Ar-H), 7.59 (s, 1H,  $=\text{CH-OCH}_3$ ), 7.78–7.80 (m, 2H, Ar-H);  $^{13}\text{C}$  NMR (100 MHz,  $d_6$ -DMSO)  $\delta$ : 191.0, 166.9, 162.8, 160.8, 160.1, 157.6, 135.1, 132.3, 131.9, 131.2, 130.1, 130.0, 129.5, 127.7, 127.6, 124.7, 124.6, 116.2, 116.0, 114.8, 108.6, 67.9, 61.8, 51.3; HRMS (MALDI) calcd for  $\text{C}_{25}\text{H}_{21}\text{FO}_5$   $[\text{M} + \text{Na}]^+$  443.1265, found 443.1278.

**(E)-Methyl-2-(2-(((3-chlorobenzoyl)phenoxy)-methyl)phenyl)-3-methoxyacrylate (2g)** Yield 65%. Yellow oil.  $^1\text{H}$  NMR (600 MHz,  $\text{CDCl}_3$ )  $\delta$ : 3.71 (s, 3H,  $\text{COOCH}_3$ ), 3.83 (s, 3H,  $=\text{CH-OCH}_3$ ), 5.06 (s, 2H,  $\text{CH}_2$ ), 6.96 (d,  $J=8.8$  Hz, 2H, Ar-H), 7.19–7.20 (m, 1H, Ar-H), 7.33–7.35 (m, 2H, Ar-H), 7.44 (d,  $J=8.4$  Hz, 2H, Ar-H), 7.51–7.53 (m, 1H, Ar-H), 7.60 (s, 1H,  $=\text{CH-OCH}_3$ ), 7.70 (d,  $J=8.4$  Hz, 2H, Ar-H), 7.75 (d,  $J=8.4$  Hz, 2H, Ar-H);  $^{13}\text{C}$  NMR (100 MHz,  $d_6$ -DMSO)  $\delta$ : 193.1, 166.8, 162.1, 160.7, 136.9, 136.3, 135.1, 132.1, 132.0, 131.1, 130.0, 129.1, 128.5, 127.6, 127.5, 114.5, 108.6, 67.8, 61.8, 51.2; HRMS (MALDI) calcd for  $\text{C}_{25}\text{H}_{21}\text{ClO}_5$   $[\text{M} + \text{Na}]^+$  459.0970, found 459.0971.

**(E)-Methyl-2-(2-(((3-benzoylphenyl)amino)methyl)phenyl)-3-methoxyacrylate (2h)** Yield 67%. Yellow oil.  $^1\text{H}$  NMR (600 MHz,  $d_6$ -DMSO)  $\delta$ : 3.70 (s, 3H,  $\text{COOCH}_3$ ), 3.83 (s, 3H,  $=\text{CH-OCH}_3$ ), 4.24 (s, 2H,  $\text{CH}_2$ ), 6.56 (d,  $J=8.4$  Hz, 2H, Ar-H), 7.16–7.17 (m, 1H, Ar-H), 7.32–7.33 (m, 2H, Ar-H), 7.41–7.45 (m, 3H, Ar-H), 7.50–7.53 (m, 1H, Ar-H), 7.57 (s, 1H,  $=\text{CH-OCH}_3$ ), 7.70–7.73 (m, 4H, Ar-H);  $^{13}\text{C}$  NMR (100 MHz,  $d_6$ -DMSO)  $\delta$ : 193.4, 167.0, 160.8, 152.8, 139.0, 137.7, 132.4, 131.9, 131.1, 128.8, 128.2, 127.6, 126.5, 126.2, 124.0, 111.1, 108.9, 61.8, 51.3, 43.7; HRMS (MALDI) calcd for  $\text{C}_{25}\text{H}_{23}\text{NO}_4$   $[\text{M} + \text{Na}]^+$  423.1519, found 423.1895.

**(E)-Methyl-2-(2-(((3-benzoylphenyl)(methyl)-amino)methyl)phenyl)-3-methoxyacrylate (2i)** Yield 68%. Yellow oil.  $^1\text{H}$  NMR (600 MHz,  $d_6$ -DMSO)  $\delta$ : 2.93 (s, 3H,  $\text{N-CH}_3$ ), 3.49 (s, 3H,  $\text{COOCH}_3$ ), 3.70 (s, 3H,  $=\text{CH-OCH}_3$ ), 4.28 (s, 2H,  $\text{CH}_2$ ), 6.78–6.81 (m, 2H, Ar-H), 6.88 (s, 1H, Ar-H), 6.96–6.99 (m, 2H, Ar-H), 7.12–7.20 (m, 3H, Ar-H), 7.37–7.39 (m, 2H, Ar-H), 7.51–7.54 (m, 2H, Ar-H and  $=\text{CH-OCH}_3$ ), 7.59–7.60 (m, 2H, Ar-H);  $^{13}\text{C}$  NMR (100 MHz,  $d_6$ -DMSO)  $\delta$ : 196.2, 166.9, 160.5, 148.9, 137.7, 137.2, 136.9, 132.4, 131.8, 131.3, 129.5, 129.0, 128.4, 127.5, 126.4, 125.6, 117.4, 115.7, 111.9, 108.8, 61.8, 53.6, 51.2, 38.7; HRMS (MALDI) calcd for  $\text{C}_{26}\text{H}_{25}\text{NO}_4$   $[\text{M} + \text{Na}]^+$  438.1676, found 438.1680.

**(E)-Methyl-3-methoxy-2-(2-(((9-oxo-9H-fluoren-2-yl)oxy)methyl)phenyl)acrylate (2j)** Yield 80%. Red solid, m.p. 132–133 °C.  $^1\text{H}$  NMR (600 MHz,  $d_6$ -DMSO)  $\delta$ : 3.63 (s, 3H,  $\text{COOCH}_3$ ), 3.85 (s, 3H,  $=\text{CH-OCH}_3$ ), 5.01 (s, 2H,  $\text{CH}_2$ ), 7.01 (s, 1H, Ar-H), 7.10–7.13 (m, 2H, Ar-H), 7.26–7.33 (m, 3H, Ar-H),

7.46–7.47 (m, 1H, Ar-H), 7.53–7.56 (m, 2H, Ar-H), 7.66–7.68 (m, 3H, Ar-H and  $=\text{CH-OCH}_3$ );  $^{13}\text{C}$  NMR (100 MHz,  $d_6$ -DMSO)  $\delta$ : 192.7, 166.8, 160.7, 159.5, 144.2, 136.4, 135.4, 134.9, 133.3, 131.9, 131.1, 128.1, 127.5, 127.4, 127.2, 123.8, 122.2, 121.0, 120.2, 110.0, 108.6, 67.9, 61.8, 51.2; HRMS (MALDI) calcd for  $\text{C}_{25}\text{H}_{20}\text{O}_5$   $[\text{M} + \text{Na}]^+$  423.1203, found 423.1321.

### Enzyme inhibition kinetic activity

The preparation of succinate-cytochrome *c* reductase (SCR, mixture of respiratory complex II and  $bc_1$  complex) from porcine heart was essentially same as reported.<sup>[12]</sup> The activity of SCR was measured by monitoring the increase of cytochrome *c* at 550 nm, by using the extinction coefficient of  $18.5 \text{ mmol} \cdot \text{L}^{-1} \cdot \text{cm}^{-1}$ . The succinate-ubiquinone reductase (complex II) activity was measured by monitoring the decrease of 2,6-dichlorophenolindophenol (DCIP) at 600 nm, by using the extinction coefficient of  $21 \text{ mmol} \cdot \text{L}^{-1} \cdot \text{cm}^{-1}$ . The reaction mixture may be scaled down to 1.8 mL with final concentrations of PBS (pH 7.4), 100 mmol/L; EDTA, 0.3 mmol/L; succinate, 20 mmol/L; oxidized cytochrome *c*, 60  $\mu\text{mol/L}$  (or DCIP, 53  $\mu\text{mol} \cdot \text{L}^{-1}$ ); and an appropriate amounts of enzyme.<sup>[13]</sup>

The ubiquinol-cytochrome *c* reductase ( $bc_1$  complex) activity in catalyzing the oxidation of  $\text{DBH}_2$  by cytochrome *c* was assayed in 100 mmol/L PBS (pH 6.5), 2 mmol/L EDTA, 750  $\mu\text{mol/L}$  lauryl maltoside (*n*-dodecyl- $\beta$ -D-maltoside), 20–120  $\mu\text{mol/L}$   $\text{DBH}_2$ , 100  $\mu\text{mol/L}$  oxidized cytochrome *c*, and an appropriate amount of SCR.<sup>[14]</sup> The preparation of  $\text{DBH}_2$  from DB was carried out according to the procedure described in previous publications,<sup>[15,16]</sup> and the concentration of  $\text{DBH}_2$  was determined by measuring the absorbance difference between 288 and 320 nm using an extinction coefficient of  $4.14 \text{ mmol} \cdot \text{L}^{-1} \cdot \text{cm}^{-1}$  for the calculation.<sup>[17,18]</sup> The nonionic detergent lauryl maltoside was used to decrease the interfering nonenzymatic activity,<sup>[8,17,18]</sup> though it was expected to affect the  $K_m$  value of  $\text{DBH}_2$  to  $bc_1$  complex. For each reaction, the nonenzymatic rate for cytochrome *c* reduction was followed for at least 100 s before enzyme was added to initiate the reaction.

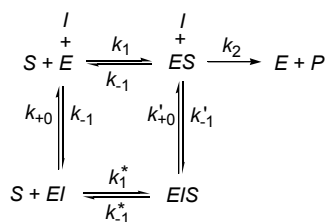
For the inhibitory kinetic studies, the reaction was carried out in the presence of varying concentrations of the inhibitor. All of the reactions were initiated by the addition of enzyme and monitored continuously by following the absorbance change at certain wavelengths on a Perkin-Elmer Lambda 45 spectrophotometer equipped with a magnetic stirrer at 23 °C.

Determination of Michaelis-Menten parameters  $K_m$  and  $V_{\text{max}}$  was performed by nonlinear regression. The inhibition type was assayed by the Lineweaver-Burk plot, and the kinetic parameters were evaluated by Sigma Plot software 9.0 for the classical inhibitors.

For slow, tight-binding inhibitors, the reaction mechanism could be considered as shown in Scheme 2, where *E*, *S*, and *I* represent enzyme, substrate, and in-

hibitor, respectively. The progress curves at different inhibitor concentrations can be described by Eq. 1.<sup>[14]</sup>

**Scheme 2** Kinetic model used for the present study



$$[P] = v_s t + \frac{v_0 - v_s}{k_{\text{obs}}} (1 - e^{-k_{\text{obs}} t}) \quad (1)$$

The data were analyzed using the nonlinear regression program of Sigma Plot 9.0 to give the individual parameters for each progress curve;  $v_0$  (initial velocity),  $v_s$  (steady-state velocity),  $k_{\text{obs}}$  (apparent first-order rate constant for the transition from  $v_0$  to  $v_s$ ) according to Eq. 1. Usually,  $k_{\text{obs}}$  constant:

$$k_{\text{obs}} = A[I]_0 + B$$

$$A = \frac{k_{+0}K_m + k_{+0}'[S]}{K_m + [S]}$$

$$B = \frac{k_{-0}K_m^* + k_{-0}'[S]}{K_m^* + [S]}$$

We have  $K_m$  and  $K_m^*$  as the Michaelis-Menten constants:

$$K_m = \frac{k_{-1} + k_2}{k_1}$$

$$K_m^* = \frac{k_{-1}'}{k_1'}$$

Like the classical inhibitors, the slow, tight-binding inhibitors can also be classified as competitive, non-competitive, and uncompetitive on the basis of similar considerations. Experimentally, the type of inhibition can be ascertained by studying the effect of  $[S]$  on the apparent rate constants  $A$  and  $B$ :

Competitive:

$$A = \frac{k_{+0}K_m}{K_m + [S]} \quad B = k_{-0} \quad (2)$$

Noncompetitive:

$$A = k_{+0}, \quad B = k_{-0} \quad (3)$$

Uncompetitive:

$$A = \frac{k_{+0}'[S]}{K_m + [S]} \quad B = \frac{k_{-0}'[S]}{K_m^* + [S]} \quad (4)$$

## Computational methods

The three dimensional (3D) structure of the porcine  $bc_1$  was obtained from our previous work.<sup>[14]</sup> The AutoDock 4.0 program was applied to dock these benzophenone-based strobilurins into the  $Q_0$  site of  $bc_1$  complex. The parameters used in molecular docking were the same as our previous work used.<sup>[14]</sup> All the complex structures derived from molecular docking were used as starting structures for further energy minimizations using the Sander module of the Amber8 program before the final binding structures were obtained. The atomic charges used for these inhibitors were the restrained electrostatic potential (RESP) charges, determined by using the standard RESP procedure implemented in the Antechamber module of the Amber8 program following the electronic structure and electrostatic potential calculations at the HF/6-31G\* level. First, the ligand was minimized with the protein fixed. Then, the backbone atoms of the protein were fixed and the other atoms were relaxed to be minimized. The final minimization was performed with both the ligand and protein relaxed. In each step, the energy minimization was executed by using the steepest descent method for the first 2000 cycles and the conjugated gradient method for the subsequent 3000 cycles with a convergence criterion of  $0.1 \text{ kcal} \cdot \text{mol}^{-1} \cdot \text{\AA}^{-1}$ . Finally, the 20 ps MD simulation was carried out for each complex structure. For temperature regulation, the Langevin thermostat was used to maintain at 300 K. The atomic coordinates were saved per ps. The last snapshot of the MD simulation was minimized to a convergence criterion of  $0.1 \text{ kcal} \cdot \text{mol}^{-1} \cdot \text{\AA}^{-1}$ . The enthalpy was calculated using MM/PBSA method and entropy was calculated as our recent publications described.<sup>[19,20]</sup> The result was shown in Table 1.

## Evaluation of fungicidal activity

The *in vivo* fungicidal activities of compounds **2a**—**2j** against cucumber *Sphaerotheca fuliginea* were tested according to the procedure described previously.<sup>[20]</sup> The results are listed in Table 2, in which the inhibition percentage was calculated by averaging the values obtained in three independent experiments. Azoxystrobin, a commercial fungicide, was used as control.

## Results and Discussion

### Synthetic chemistry

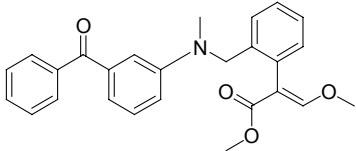
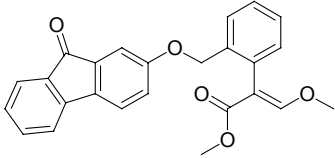
The synthetic route for the target compounds is outlined in Scheme 1. The key intermediate (*E*)-methyl-2-

**Table 1** Inhibitory activities of compounds **2a–2j** against porcine SCR with cytochrome *c* as substrate

No.	Structure	$K_i/(\text{nmol}\cdot\text{L}^{-1})$	$\Delta H/(\text{kcal}\cdot\text{mol}^{-1})$	$-T\Delta S/(\text{kcal}\cdot\text{mol}^{-1})$	$\Delta G/(\text{kcal}\cdot\text{mol}^{-1})$		Residue interaction energy/ ( $\text{kcal}\cdot\text{mol}^{-1}$ )	
					cal.	exp.	F274	F128
<b>2a</b>		13.95	−50.00	19.94	−30.06	−10.74	−7.130	−7.345
<b>2b</b>		3.28	−51.63	19.14	−32.49	−11.60	−10.472	−6.872
<b>2c</b>		>1000	—	—	—	—	—	—
<b>2d</b>		>1000	—	—	—	—	—	—
<b>2e</b>		12.49	−49.93	19.40	−30.53	−10.82	−7.629	−5.258
<b>2f</b>		16.87	−46.70	17.59	−29.11	−10.63	−6.042	−8.175
<b>2g</b>		10.35	−49.21	17.70	−31.51	−10.92	−8.377	−5.555
<b>2h</b>		>1000	—	—	—	—	—	—



Continued

No.	Structure	$K_i/(\text{nmol}\cdot\text{L}^{-1})$	$\Delta H/(\text{kcal}\cdot\text{mol}^{-1})$	$-T\Delta S/(\text{kcal}\cdot\text{mol}^{-1})$	$\Delta G/(\text{kcal}\cdot\text{mol}^{-1})$		Residue interaction energy/ ( $\text{kcal}\cdot\text{mol}^{-1}$ )	
					cal.	exp.	F274	F128
2i		>1000	—	—	—	—	—	—
2j		1.89	-50.90	18.25	-32.65	-11.93	-9.14	-6.44
AZ	—	297.60	-43.42	19.42	-23.00	-8.92	-8.96	-4.29

**Table 2** *In vivo* fungicidal activities of compounds **2a–2j** and AZ

200 mg/L (Inhibition rate, %)			
No.	<i>S. fuliginea</i>	No.	<i>S. fuliginea</i>
2a	0	2g	96
2b	93	2h	0
2c	0	2i	0
2d	0	2j	80
2e	56	AZ	85
2f	43		

(2-(bromomethyl)phenyl)-3-methoxyacrylate (**3**) was prepared according to the existing method.<sup>[6]</sup> Then, compound **3** reacted with various benzophenones **4** or 2-hydroxy-9H-fluoren-9-one (**5**) to afford the target compounds **2a–2h** and **2j** in yields of 65%–81%. Compound **2i** was prepared by the *N*-methylation of **2c** in a yield of 68%. The structures of all the target compounds were characterized by <sup>1</sup>H NMR, <sup>13</sup>C NMR and HRMS spectra.

### Cytochrome *bc*<sub>1</sub> inhibition activity

As shown in Table 1, six compounds (**2a**, **2b**, **2e**, **2f**, **2g**, and **2j**) were found to exhibit higher (from 21-fold to 157-fold) inhibitory activities against the porcine cytochrome *bc*<sub>1</sub> complex than the control of azoxystrobin, whereas compounds **2c**, **2d**, **2h**, and **2i** showed very low inhibition effects against porcine cytochrome *bc*<sub>1</sub> complex. In addition, the O-bridged derivatives **2b** ( $K_i = 3.28$  nmol/L) is more active than its corresponding S-bridged derivative **2a** ( $K_i = 13.95$  nmol/L) and the NH-bridged derivative **2c** ( $K_i > 1000$  nmol/L). Besides, compounds **2e**, **2f** and **2g** showed comparable potency as compound **2a**, indicating that substitution on the benzophenone as pharmacophore has not significant

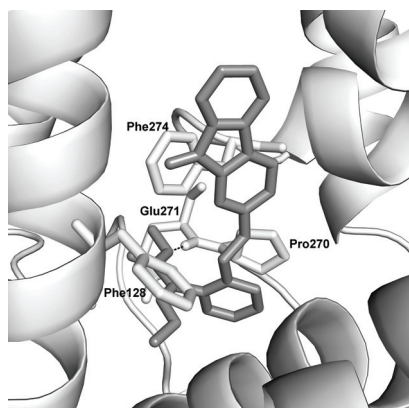
effect on the activity.

Table 1 also summarizes the  $K_i$  values against the porcine *bc*<sub>1</sub> complex for the inhibition by the synthesized compounds and also by the commercial compound azoxystrobin that was used as the control. Interestingly, the calculated binding free energies correlated reasonably well with the binding free energies derived from the corresponding experimental  $K_i$  values with a correlation coefficient of  $r^2 = 0.89$ , confirming the reliability of our computational models. As shown in Table 1, compound **2j** distinguishes itself as the most promising candidate with the highest potency ( $K_i = 1.89$  nmol/L), with about 157-fold improved binding affinity compared to AZ.

Figure 3 showed the simulated binding model of compound **2j**, from which we can conclude that the pharmacophore of this new inhibitor bound in the fashion of typical MOA inhibitors. It bounded with Phe128, Tyr131, Phe274, and Glu271, formed a H-bond between the methoxy of the methoxyacrylate and the backbone N of Glu271. Very importantly, the  $\pi$ - $\pi$  interactions between Phe274 and the fluorenone ring of compound **2j** were improved significantly compared with that of azoxystrobin, which accounts for the higher potency of compound **2j**.

### Enzymatic kinetics

As shown in Figure 4A illustrating progress curves, compound **2j** exhibits slow-binding behavior to porcine *bc*<sub>1</sub> complex. Over a time period in which the uninhibited enzyme displays a simple linear progress curve like line 1 in Figure 4A, the data in the presence of **2j** will display a quasi-linear relationship with time in the early part of the curve, converting later to a slower linear relationship between product and time. Increasing the concentration of **2j** led to the decrease of the steady-state rate ( $v_s$ ) in the progress curve and the progress curves obtained using various concentrations of **2j**



**Figure 3** Simulated binding model of compound **2j** (gray) in  $bc_1$  complex (light gray).

were fitted to Eq. 1 to determine  $v_0$ ,  $v_s$  and  $k_{\text{obs}}$ . The  $k_{\text{obs}}$  values were respectively 0.0298, 0.0333, 0.0469, 0.0944 and  $0.1740 \text{ s}^{-1}$  when the concentrations of **2j** were respectively 1, 2.5, 5, 10 and 20 nmol/L. The plot for  $k_{\text{obs}}$  versus  $[I]$  is shown in Figure 4B.  $k_{\text{obs}}$  is proportional to the inhibitor concentration, the slope corresponds to the apparent rate constants  $A = (0.0079 \pm 0.0004) \text{ s}^{-1} \cdot \text{nmol}^{-1}$  and the intercept corresponds to the apparent rate constants  $B = (0.015 \pm 0.004) \text{ s}^{-1}$ .

To distinguish the mode of inhibition of a time-dependent inhibitor, it is convenient to analyze the effect of various substrate concentrations on  $k_{\text{obs}}$  at fixed inhibitor concentration. A competitive-type inhibitor will display a decrease of  $k_{\text{obs}}$  with increasing substrate concentration. In contrast, with uncompetitive inhibitors the value of  $k_{\text{obs}}$  will increase with increasing substrate concentration, while  $k_{\text{obs}}$  is independent of substrate concentration for noncompetitive-type inhibition. So we monitored the time courses of the  $bc_1$  complex-catalyzed reaction in the presence of different concentrations of cytochrome *c* and at a fixed concentration of **2j** (Figure 5A). The values of  $k_{\text{obs}}$  can be obtained by fitting the progress curves according to the substrate reaction kinetic theory and are plotted against the concentration of cytochrome *c* in Figure 5B. The data clearly revealed that  $k_{\text{obs}}$  was independent of the concentration of substrate cytochrome *c*, indicating that **2j** is a noncompetitive inhibitor with respect to cytochrome *c*. Thus,

the values of  $A$  and  $B$  determined from Figure 4B are equal to the true association and dissociation rate constants  $k_{+0}$  and  $k_{-0}$  according to Eq. 3, respectively, and the inhibition constant for **2j** can be calculated as  $K_i = k_{-0}/k_{+0} = (1.8987 \pm 0.0432) \text{ nmol/L}$ .

In order to study the effect of substrate ubiquinol on the inhibition kinetics of **2j**, the  $bc_1$  complex activity of SCR was further measured directly by using decylubiquinol ( $\text{DBH}_2$ ) or cytochrome *c* as substrates in the absence and in the presence of **2j**. In the presence of **2j**, with succinate used as substrate, the progress curves exhibited a similar curvilinear (Figure 6A and 6B). However, when the experiments were performed at a fixed concentration of **2j**, the  $k_{\text{obs}}$  value decreased with increasing concentration of  $\text{DBH}_2$ , which is different from what is observed in Figure 5B. To further elucidate the inhibitory mechanism, we carried out six sets of inhibitory experiments in the presence of varying concentrations of  $\text{DBH}_2$  and **2j**. Similarly, from these progress curves of product formation at fixed concentrations of  $\text{DBH}_2$ , the values of  $v_0$ ,  $v_s$  and  $k_{\text{obs}}$  can be determined as described previously. Plots of  $k_{\text{obs}}$  against the inhibitor concentration give a straight line (insets of Figure 6A and 6B), from which the values of  $A$  (slope) and  $B$  (intercept) at indicated  $\text{DBH}_2$  concentrations were obtained. Figures 6C and 6D show the dependence of the  $A$  and  $B$  values on the  $\text{DBH}_2$  concentration. Clearly,  $A$  decreased with increasing the concentration of  $\text{DBH}_2$ , while  $B$  was not influenced, suggesting that **2j** is a competitive inhibitor with respect to substrate ubiquinol. Thus, the microscopic inhibition rate constants  $k_{+0} = (0.3713 \pm 0.0259) \text{ s}^{-1} \cdot \text{nmol} \cdot \text{L}^{-1}$  and  $k_{-0} = (0.0018 \pm 0.0003) \text{ s}^{-1}$  can be obtained by fitting Eq. 2 to the experimental data, and the inhibition constant  $K_i = k_{-0}/k_{+0} = (4.848 \pm 0.316) \text{ nmol/L}$  can be derived. The  $K_i$  value determined is about 2.55-fold higher than that measured from the succinate-cytochrome *c* reductase activity inhibition, which is mainly due to the presence of lauryl maltoside since increasing the concentration of lauryl maltoside, the  $k_{\text{obs}}$  value will be decreased.

### Fungicidal activity

The *in vivo* fungicidal activities of all the new compounds against *S. fuliginea* were screened. As listed in

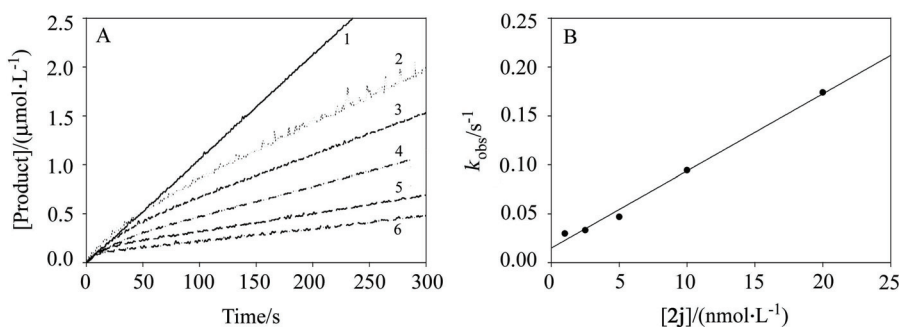


**Figure 4** (A) Inhibitory kinetics of  $bc_1$  complex by **2j**. Each reaction mixture contains 100 mmol/L PBS (pH 7.4), 0.3 mmol/L EDTA, 20 mmol/L succinate, 100  $\mu\text{mol/L}$  cytochrome *c*, 0.1 nmol/L SCR, and a certain amount of **2j** (1, 0 nmol/L; 2, 1 nmol/L; 3, 2.5 nmol/L; 4, 5 nmol/L; 5, 10 nmol/L and 6, 20 nmol/L). (B) Plot of  $k_{\text{obs}}$  against concentration of **2j**.



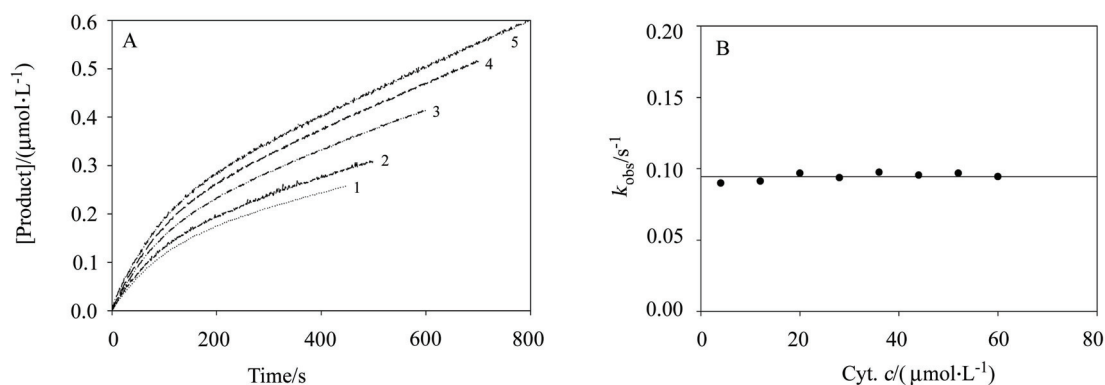


**Figure 5** (A) Effect of cytochrome *c* concentration on the inhibition of *bc*<sub>1</sub> complex by **2j**. The assays were carried out in the presence of 10 nmol/L **2j** and various concentrations of cytochrome *c* (1, 12 μmol/L; 2, 20 μmol/L; 3, 28 μmol/L; 4, 44 μmol/L and 5, 60 μmol/L). Each reaction was initiated by adding 0.1 nmol/L SCR. (B) Plot of  $k_{\text{obs}}$  against concentration of cytochrome *c*.

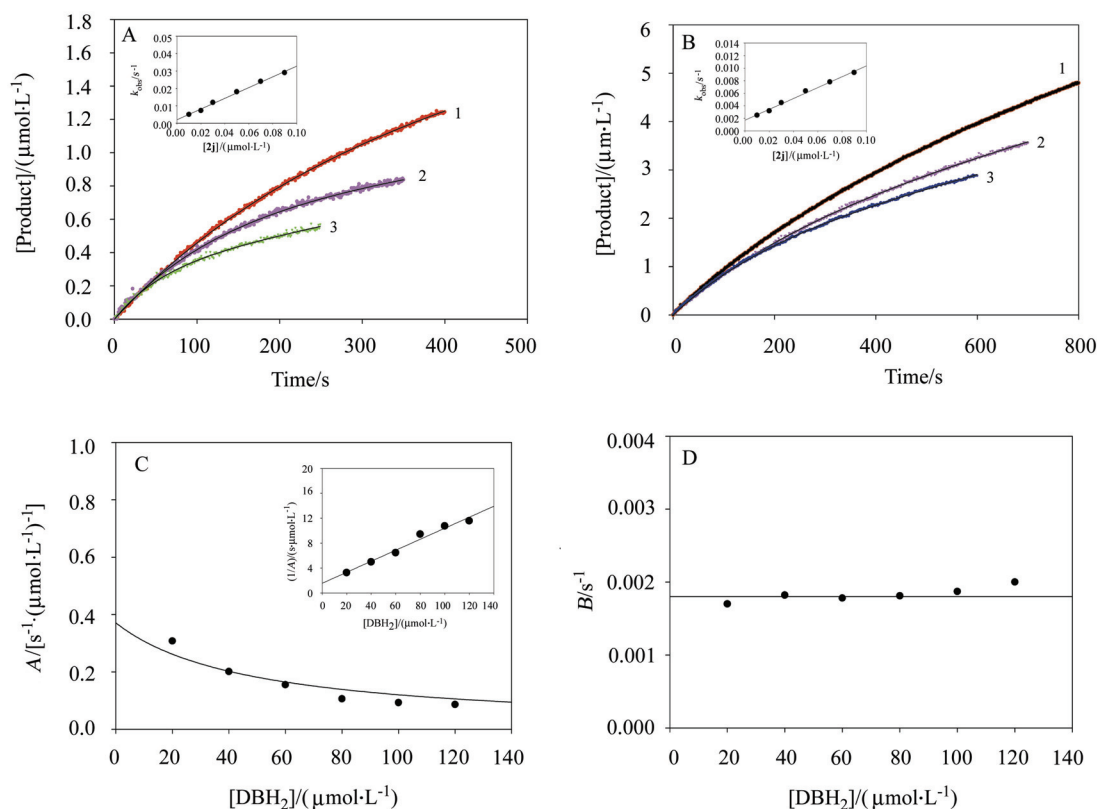


**Figure 6** (A, B) Inhibitory kinetics of porcine *bc*<sub>1</sub> complex by **2j**. Each reaction mixture contains 100 mmol/L PBS (pH 6.5), 2 mmol/L EDTA, 750 μmol/L lauryl maltoside, 100 μmol/L oxidized cytochrome *c*, 0.05 nmol/L SCR, a certain amount of DBH<sub>2</sub> (A, 20 μmol/L; B, 120 μmol/L), and **2j** (1, 10 nmol/L; 2, 20 nmol/L and 3, 30 nmol/L). Experimental data are shown as dots and theoretical values as lines. Insets: Plots of  $k_{\text{obs}}$  against concentration of **2j**. (C) Plot of the apparent rate constant *A* against concentration of DBH<sub>2</sub>. Inset: Plot of  $1/A$  against concentration of DBH<sub>2</sub>. (D) Plot of the apparent rate constant *B* against concentration of DBH<sub>2</sub>.

Table 2, some compounds exhibited significant fungicidal activity against *S. fuliginea* at the concentration of 200 mg/L, and overall, the order of the fungicidal activity is *m*-benzophenone derivative > *p*-benzophenone derivative > *o*-benzophenone derivative. Among them, compound **2j**, a *m*-benzophenone derivative, displayed the same level of fungicidal activity as azoxystrobin. Most importantly, compounds **2b** and **2g** showed higher fungicidal activity than azoxystrobin, which indicates

that benzophenone-containing derivatives worth further investigation.

## Conclusions

In summary, we have successfully designed and synthesized a series of benzophenone/fluorenone-containing derivatives **2a–2j** as inhibitors of cytochrome *bc*<sub>1</sub> complex. Very promisingly, compound **2j** with a  $K_i$

value of 1.89 nmol/L was found to display about 157-fold improved binding affinity compared to the commercial inhibitor azoxystrobin. The further inhibitory kinetics studies revealed that compound **2j** is a non-competitive inhibitor with respect to substrate cytochrome *c*, but is a competitive inhibitor with respect to substrate ubiquinol. The present work demonstrated that strobilurin analogues containing benzophenone or fluorenone side chain could be used as new leads for future fungicide discovery. Further structural optimization and *in vivo* fungicidal activities about benzophenone-based strobilurin derivatives are well under way.

## Acknowledgement

The research was supported in part by the National Basic Research Program of China (No. 2010CB126103), the NSFC (Nos. 20902034, 20925206 and 21102052) and the National Key Technologies R&D Program (No. 2011BAE06B05).

## References

- [1] Kim, H.; Xia, D.; Yu, C. A.; Xia, J. Z.; Kachurin, A. M.; Zhang, L.; Yu, L.; Deisenhofer, J. *Proc. Natl. Acad. Sci. U. S. A.* **1998**, *95*, 8026.
- [2] Gao, X.; Wen, X.; Yu, C. A.; Esser, L.; Tsao, S.; Quinn, B.; Zhang, L.; Yu, L.; Xia, D. *Biochemistry* **2002**, *41*, 11692.
- [3] Berry, E. A.; Huang, L. *FEBS Lett.* **2003**, *555*, 13.
- [4] Esser, L.; Quinn, B.; Li, Y. F.; Zhang, M.; Elberry, M.; Yu, L.; Yu, C. A.; Xia, D. *J. Mol. Biol.* **2004**, *341*, 281.
- [5] Beautelement, K.; Clough, J. M.; de Fraine, P. J.; Godfrey, C. R. A. *J. Pestic. Sci.* **1991**, *31*, 499.
- [6] Zhao, P. L.; Liu, C. L.; Huang, W.; Wang, Y. Z.; Yang, G. F. *J. Agric. Food Chem.* **2007**, *55*, 5697.
- [7] Huang, W.; Zhao, P. L.; Liu, C. L.; Chen, Q.; Liu, Z. M.; Yang, G. F. *J. Agric. Food Chem.* **2007**, *55*, 3004.
- [8] Fisher, N.; Meunier, B. *Pest Manag. Sci.* **2005**, *61*, 973.
- [9] Gisi, U.; Sierotzki, H.; Cook, A.; McCaffery, A. *Pest Manag. Sci.* **2002**, *58*, 859.
- [10] Hao, G.-F.; Wang, F.; Li, H.; Zhu, X.-L.; Yang, W.-C.; Huang, L.-S.; Wu, J.-W.; Berry, E. A.; Yang, G.-F. *J. Am. Chem. Soc.* **2012**, *134*, 11168.
- [11] Worthington, P. A. *J. Pestic. Sci.* **1991**, *31*, 457.
- [12] Yu, L.; Yu, C. *J. Biol. Chem.* **1982**, *257*, 2016.
- [13] King, T. E. *Methods Enzymol.* **1967**, *10*, 216.
- [14] Zhao, P. L.; Wang, L.; Zhu, X. L.; Huang, X.; Zhan, C. G.; Wu, J. W.; Yang, G. F. *J. Am. Chem. Soc.* **2010**, *132*, 185.
- [15] Rieske, J. S. *Methods Enzymol.* **1967**, *10*, 239.
- [16] Luo, C.; Long, J.; Liu, J. *Clin. Chim. Acta* **2008**, *395*(1–2), 38.
- [17] Fisher, N.; Bourges, I.; Hill, P.; Brasseur, G.; Meunier, B. *Eur. J. Biochem.* **2004**, *271*, 1292.
- [18] Fisher, N.; Brown, A. C.; Sexton, G.; Cook, A.; Windass, J. *Eur. J. Biochem.* **2004**, *271*, 2264.
- [19] Pan, Y.; Gao, D.; Zhan, C. G. *J. Am. Chem. Soc.* **2008**, *130*, 5140.
- [20] Zhu, X. L.; Yang, W. C.; Yu, N. X.; Yang, S. G.; Yang, G. F. *J. Mol. Model.* **2011**, *17*, 495.

(Pan, B.; Qin, X.)